RSC Advances

ROYAL SOCIETY OF CHEMISTRY

www.rsc.org/advances

Predictive calculation of carbon dioxide solubility in polymers

XIA Ru-Ting *[a,b], *HUANG Xing-Yuan* [b]

[a]School of Mechanical Engineering, Taizhou University, Taizhou, Zhejiang 318000,China

[b]College of Mechanical and Electric Engineering, Nanchang University, Nanchang 330029, China

ABSTRACT:

Solubility of carbon dioxide in polymer has attracted great attention of scientists because it is an important application of green chemistry, and it is widely applied in extraction, separation and preparation of new materials. In this work, a new solubility prediction model with both good accuracy and efficiency, called CEAPSO KHM RBF ANN is developed. In the CEAPSO KHM RBF ANN model, accelerated particle swarm optimization (APSO) algorithm with chaotic disturbance is employed to trim the radial basis function artificial neural network (RBF ANN) connection weights and biases in order to reduce premature convergence problem, and K-harmonic means (KHM) clustering method is used to tune the hidden centers and spreads of radial basis function. The proposed model is employed to investigate the solubility of CO_2 in polymers including Polypropylene, Polystyrene, Poly(vinyl acetate), Carboxylated polyesters and Poly(butylene succinate-co-adipate), respectively. The results indicate that the proposed model is an effective method for solubility prediction with better performance and higher efficiency compared with the other methods, and should contribute to understanding the phase behaviour of the gas/polymer system and for the design and optimization of processing techniques.

Keyword: Computational chemistry, polymers, solubility model, hybrid method.

1. Introduction

Carbon dioxide (CO_2) has become the most popular green medium currently, and has been widely used as solute or solvent in many fields including the material modification, synthesis and processing because of its advantages like no toxicity, chemical inertness, nonflammable feature and easy access[1-3]. Solubility of CO_2 in polymers has been a subject of interest for chemical engineers for several decades, it has also been applied in a wider application field, such as extraction, separation and preparation of new materials and so forth [4, 5]. To describe gas solubility in polymer, the calculation models are often used [6]. For example, thermodynamic model and intelligent model have been extended to describe phase behavior of polymer solution. The thermodynamic methods consist of equation of state, empirical equation and semi-empirical equation; while intelligent calculation methods consist of artificial neural network (ANN) and support vector machine [7-12]. Bakhbakhi [13] applies the equation of state and ANN to conduct comparison of calculation of solubility, which turns out that the computational accuracy obtained through calculation by ANN is higher; Pahlavanzadeh[14] proves that a better effect in calculation of solubility can be achieved by using ANN; Mehdizadeh[15] and Gharagheizi[16] also conclude that ANN has better performance in the prediction of solubility. Due to the good generalization ability, radial basis function (RBF) ANN has been widely used for prediction of solubility, but Khajeh[17] summaries through comparison that adaptive neuro-fuzzy inference system (ANFIS) has better performance in predicting of solubility than that of RBF ANN. In other words, the network parameters of RBF ANN have conclusive influence on the overall performance, and an optimization is necessary. As is known to all that the parameters optimization of the ANN is a classical optimization problem, so many intelligent optimization algorithms

have been used for optimization of network parameters [18], such as genetic algorithm [19-21], simulated annealing [22], particle swarm optimization (PSO) [23, 24], tabu search [25, 26], cuckoo search algorithm [27], etc.

PSO algorithm is a classical intelligence algorithm inspired by the birds seeking for food. It has many advantages, such as less adjustment parameter, convenient implementation, fast convergence speed, etc. And it has been broadly used for parameters optimization of ANN. Liu [28] has successfully obtained the prediction model of melt index of fuzzy ANN by PSO; Lazzus [29] also successfully establishes the hybrid prediction model based on PSO and ANN. However, PSO itself also has some defects, for example, poor search capability at later period of optimization and being easy to fall into local mininum. In order to improve the deficiencies, scientists have proposed many variants. Li [30-34] proposed several models applied the chaos theory and self-adaption strategy in the improvement of PSO. The results show the effects of prediction of the proposed models are pretty good.

In the past two years, a new variant called accelerated PSO (APSO) has been the simplest and high-efficiency algorithm with free parameters among so many variants, to which has been paid close attention by researchers. It has successfully solved many practical problems. Specifically, it is suitable for optimization of RBF ANN parameters. But it also has problems like being easy to fall into local minimum. Given that, this article will discuss the integration of APSO and chaos theory to propose an improved algorithm, and apply the improved algorithm and K-harmonic means (KHM) clustering in the training of RBF ANN. Consequently, it attempts to get a hybrid network model with both good accuracy and efficiency, and use the model in the prediction of solubility of CO_2 in polymer in this work.

2. Theory and Experimental Data

2.1 Chaos-enhanced accelerated particle swarm optimization

Recent years, APSO is a new simplified variant of PSO algorithm; it could accelerate the convergence using the global best only. In the APSO, the velocity is abandoned in order to increase the convergence speed even further, thus there is no need to initialize the velocity [35]. Therefore, it is much simpler to implement. The position vector of a particle is updated as follow:

$$x_i^{t+1} = (1-c_1)x_i^t + c_1 g_{best} + c_2 r \quad (1)$$

where x_i is the position vector, g_{best} is the global extremum. r is random vector, c_1 and c_2 are often called acceleration coefficients.

The APSO is very efficient, but it also has problems like being easy to fall into local minimum, and may miss some solutions sometime. In fact, there is no need to keep the acceleration coefficients as constant, and the varying acceleration coefficients are very advantageous, which may lead to the convergence speedup. Therefore, in this work, we employ the Lorenze equations to generate chaotic sequence for tuning the acceleration coefficients c_1 and c_2 of APSO, and develop a new improved algorithm, called CEAPSO. Chaotic sequence is defined as follow [36] :

$$\begin{cases} \dfrac{dx}{dt} = -a(x-y) \\ \dfrac{dy}{dt} = rx - y - xz \\ \dfrac{dz}{dt} = xy - bz \end{cases} \quad (2)$$

where a, b, and c are the system parameters, and the Lorenze system can achieve chaotic state completely when a, b, and c are set as 10, 8/3 and 28, respectively [37].

Given the dynamic properties of $x(t)$ and $y(t)$, the acceleration coefficients c_1 and c_2 are defined as follows:

$$\begin{cases} c_1 = x(t) \\ c_2 = y(t) \end{cases} \tag{3}$$

The acceleration coefficients c_1 and c_2 can enhance the ability to escape local minimum by tuning with chaotic sequence, at the same time increase the possibility of searching global extremum.

2.2 KHM Cluster Method

KHM cluster is an iterative process based on cluster center. The objective function adopts the harmonic mean of distance from all the sample points to each center of clustering, defined as:

$$KHM(X,C) = \sum_{i=1}^{n} \frac{k}{\sum_{j=1}^{k} \frac{1}{\left\| x_i - c_j \right\|^p}} \tag{4}$$

In the formula, $X = [x_1, \cdots, x_n]$ is the sample data set; *n* is the number of sample; *k* is the number of cluster; $C = [c_1, \cdots, c_n]$ is vector quantity of center of clustering;

The computational formulas of degree of membership $m(c_j / x_i)$ and weight $w(x_i)$ between each sample data and vector quantity of center of clustering are:

$$m(c_j / x_i) = \frac{\left\| x_i - c_j \right\|^{-p-2}}{\sum_{j=1}^{k} \left\| x_i - c_j \right\|^{-p-2}} \tag{5}$$

$$w(x_i) = \frac{\sum_{j=1}^{k} \left\| x_i - c_j \right\|^{-p-2}}{(\sum_{j=1}^{k} \left\| x_i - c_j \right\|^{-p})^2} \tag{6}$$

p is the input parameter, and it's assumed as 2 in this article [38].

The updated formula of vector quantity of cluster center, c_j, is:

$$c_j = \frac{\sum_{i=1}^{n} m(c_j / x_i) w(x_i) x_i}{\sum_{i=1}^{n} m(c_j / x_i) w(x_i)} \quad (7)$$

KHM clustering algorithm will constantly iterate based on the vector quantity of center of clustering and according to the original value, so as to make the value of objective function gradually reduce until being stable.

2.3 CEAPSO KHM RBF ANN

RBF ANN is one of the classical forward neural networks, containing three layers, input layer, hidden layer and output layer. This article proposes a hybrid RBF ANN model based on the CEAPSO and KHM cluster algorithm, called CEAPSO KHM RBF ANN. The output of the network model is defined as:

$$O(x_k) = \sum_{i=1}^{c} w_i g_i(x_k) \quad (8)$$

In the formula, w_i is the connection weight of the i^{th} hidden node. $x_k (1 \le k \le n)$ is the No. *k* input vector; c is the amount of node at hidden layer; g is the activation function.

The training process of RBF ANN can be regarded as a process of optimization of the center, spread and connection weight, that is, to optimize c_i, σ_i and w_i. In this article, we adopt KHM algorithm to optimize the center and spread of radial basis function, defined as:

$$KHM(C_{basis-funtion}, C_{cluster}) \quad (9)$$

In that, $C_{cluster}$ is the center of clustering in KHM algorithm; $C_{basis-funtion}$ is the center of radial basis function. The center of each radial basis function will update according to center of clustering.

In the meantime, the connection weight and bias of hidden layer and output layer in RBF ANN will be optimized by means of CEAPSO algorithm. For this, we define the structure of particle as:

$$particle(i) = [W_{h,o}, B_{h,o}] \quad (10)$$

In the formula, $W_{h,o}$ and $B_{h,o}$ $(1 \le h \le c)$, $(1 \le o \le p)$ are respectively the weight matrix and bias matrix between the hidden node *h* and output node *o*; p is the amount of output node.

2.4 Experimental Data

We collected 382 groups of experimental data, including 5 varieties of polymer, such as polypropylene(PP), Polystyrene(PS), Poly(vinyl acetate)(PVAc), Carboxylated polyesters(CPEs) and poly(butylene succinate-co-adipate)(PBSA). The experimental data have all obtained through literature collection. The data statistics are as shown in Table 1.

Table 1. Experimental data in this work

Polymer	*T (K)*	*P(Mpa)*	*S (g/g)*	Data points	Reference
PP	313.20-483.70	2.930-24.910	0.02050-0.26170	92	[39-42]
PBSA	323.15-453.15	1.098-20.127	0.01184-0.17410	58	[39, 43]
PS	170.00-473.15	2.068-44.410	0.00282-0.16056	104	[39, 44-46]
PVAc	313.15-373.15	0.199-17.449	0.00551-0.34692	39	[39, 46]
CPE55	306.00-343.00	0.140-31.020	0.00030-0.63660	30	[47]
CPE60	306.00-344.00	0.140-29.910	0.00230-0.56840	30	[47]
CPE67	309.00-343.00	0.130-31.000	0.00080-0.58950	29	[47]
total	170.00-483.70	0.199-44.410	0.00282-0.43010	382	

The sample of each polymer will be divided into 3 subsets, namely, training set, validation set and testing set; in order to completely train the model, about 70% of the data will be used for training, 15% used for validation of reliability of the model, and 15% used for testing the performance of model [48, 49].

3. Results and Discussion

In order to validate and test the performance of model, average relative deviation (*ARD*), root mean square error of prediction (*RMSEP*), and squared correlation coefficient (R^2) are selected as the criteria for the accuracy of each model and can be defined as:

$$ARD = \frac{1}{N}\sum_{i=1}^{N}\frac{\left|\overline{y}_i - y_i\right|}{y_i} \tag{11}$$

$$RMSEP = \sqrt{\frac{1}{\mathrm{N}}\sum_{\mathrm{i=1}}^{\mathrm{N}}(y_i - \overline{y}_i)^2} \tag{12}$$

$$R^2 = \frac{\left[\sum_{\mathrm{i=1}}^{\mathrm{N}}(y_i - y_{ave})(\overline{y}_i - \overline{y}_{ave})\right]^2}{\sum_{\mathrm{i=1}}^{\mathrm{N}}(y_i - y_{ave})^2\sum_{\mathrm{i=1}}^{\mathrm{N}}(\overline{y}_i - \overline{y}_{ave})^2} \tag{13}$$

In these formulas, *N* is the amount of data sample; $\overline{y}_i$ is the predicted value of model; y_i is experiment value; y_{ave} is the experimental average value and $\overline{y}_{ave}$ is the predicted average value.

3.1 Results of the proposed model

The model has selected two variables, temperature and pressure, as the input variables; and it will output the solubility predicted by the model. The amount of node in hidden layer can be obtained by trial-and-error method. 8 models will be respectively

established assuming the number of node in hidden layer from 3 to 10. Figure 1 has drawn the variation of MSE of the model with the changing amount of node in hidden layer. It can be concluded that when there are 7 nodes in the hidden layer, the minimum model error appears.

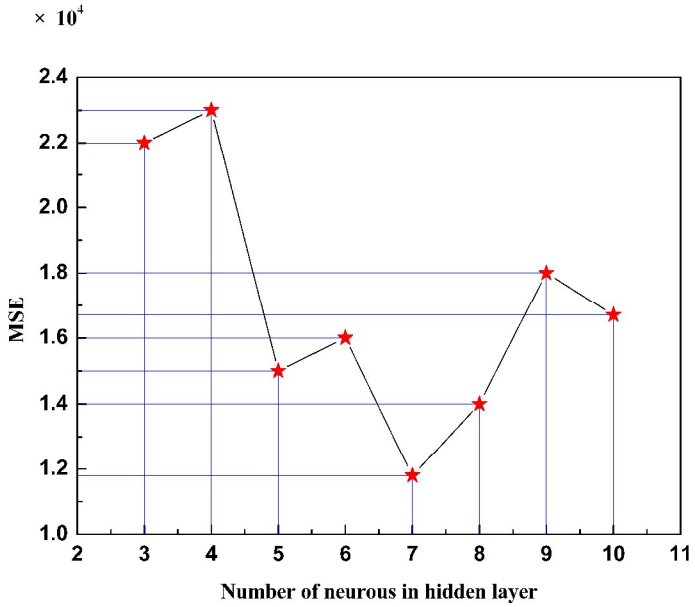

Figure 1. Results of topology studies for optimal ANN configuration

Thus, the CEAPSO KHM RBF ANN model of CO_2 solubility in polymer is developed, and the structure is 2-7-1. In Figures 2-3 the prediction of CO_2 solubility in polymers by the CEAPSO KHM RBF ANN was plotted against the experimental values for the training and validation set, in which the straight line indicates the perfect state where predicted value equals to the experimental value, and the vertical dimension between the predicted data point and the straight line presents the absolute deviation between the predicted value and experimental value. As shown in these figures, the proposed model for the training set and validation set all have good predictive ability and the vertical dimension between the predicted data point and the straight line is relatively

short, that is, the deviation between the predicted value and the experimental value is small.

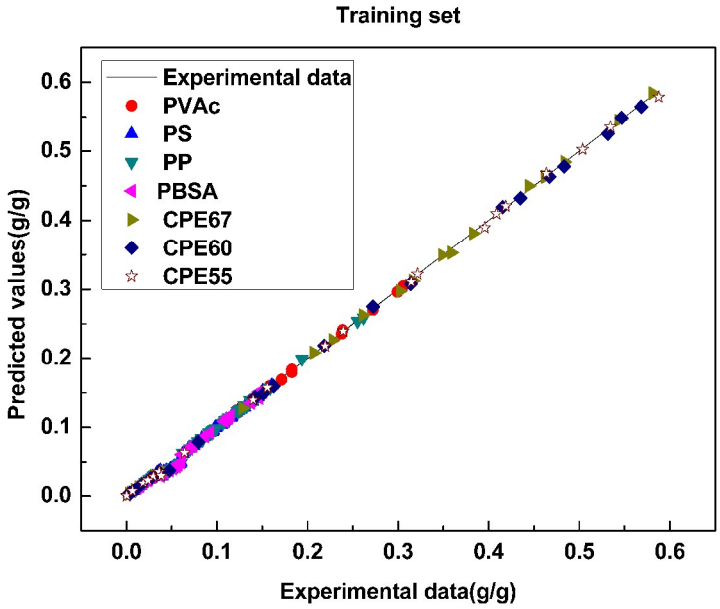

Figure 2. Predicted data versus experimental data in training set.

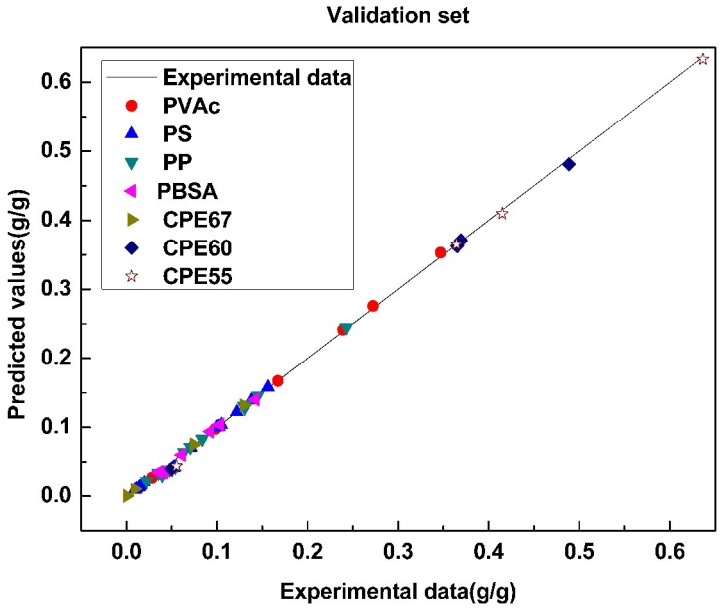

Figure 3. Predicted data versus experimental data in validation set.

Figures 4-5 plot the correlations between the predicted value and experimental value for the testing set. It can be seen from the figures that the difference between

calculated data and experimental data is very low and it is showing that the CEAPSO KHM RBF ANN model is a powerful tool for predicting of CO_2 solubility in polymers. Especially, the model performs much better on PP, CPEs and PVAc, the predicated values are almost equal to experimental values.

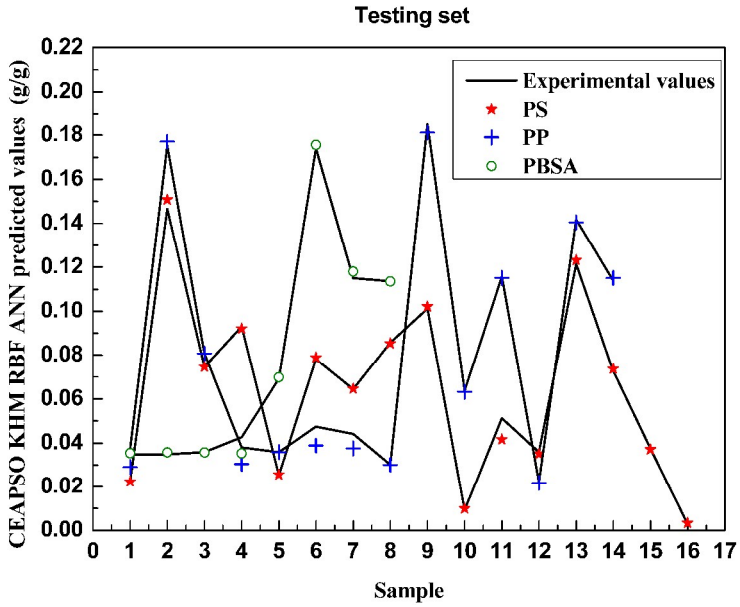

Figure 4. Predicted data versus experimental data in testing set (1).

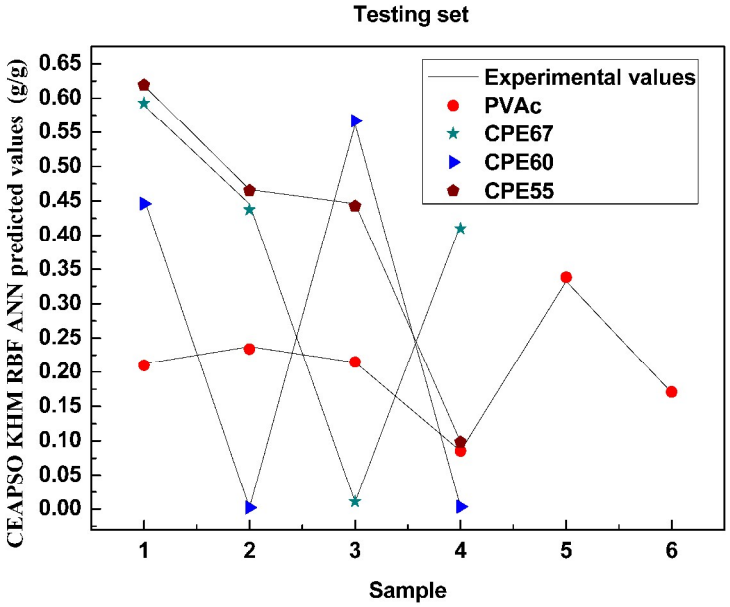

Figure 5. Predicted data versus experimental data in testing set (2).

Table 2 gives the statistical data of prediction on various polymers in the testing set. The results show that the model can accurately predict the solubility of CO_2 in polymers, and the output of the model is relatively identical with the expectation. Table 2 also indicates that both the prediction accuracy and correlation of model have performed good combination property.

Table 2. Values of ARD, R^2 and RMSEP in the testing set

Polymer	*ARD*	R^2	*RMSEP*
PVAc	0.1035	0.9959	0.0104
PS	0.1028	0.9978	0.0106
PP	0.1013	0.9987	0.0105
PBSA	0.1029	0.9984	0.0106
CPE55	0.0956	0.9991	0.0102
CPE60	0.0962	0.9987	0.0101
CPE67	0.0987	0.9985	0.0102
Average	0.1001	0.9982	0.0104

3.2 Comparative results

Firstly, two models of the same variety, PSO RBF ANN and CEAPSO RBF ANN, are selected as comparative models in order to validate the combination property of these models. Comparison among these models is not an easy task because all of these models are based on same data. In fact, a fair comparison is only achieved when all the models are constructed on the same data set. Thereupon, we randomly selected 10 data points from each polymer to get a database with 70 data points for the comparison. Figure 6 shows the convergence curves of each model. It can be concluded from the figure that the convergence rate of each model is normal. The CEAPSO KHM RBF ANN model achieves stable convergence upon the 100^{th} iteration

approximately, and the CEAPSO RBF ANN model is also gradually become stable upon the 180th iteration. However, in terms of the convergence precision, the model proposed in this work is better than the other models.

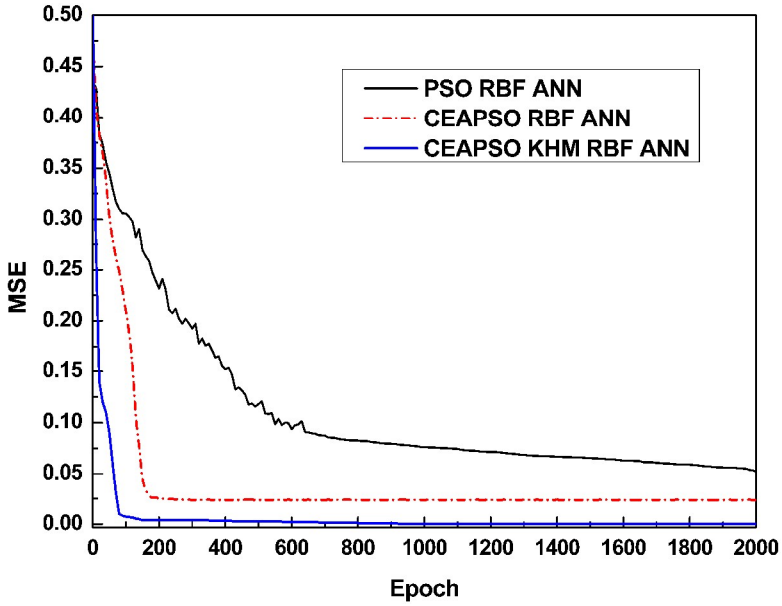

Figure 6. Curve of MSE VS. Epoch

Figure 7 shows the comparison between predicted solubility and experimental values of each model. As we can see from this figure, the distance between the predicated data point and the straight line of the model proposed in this work is small. It means that the predicated data points are mostly falling near the straight line, the predicated values are nearly identical with the experimental values, and the prediction error is relatively small. The figure shows that good agreement is obtained with the CEAPSO KHM RBF ANN model while the performance of the CEAPSO RBF ANN and PSO RBF ANN are less satisfactory.

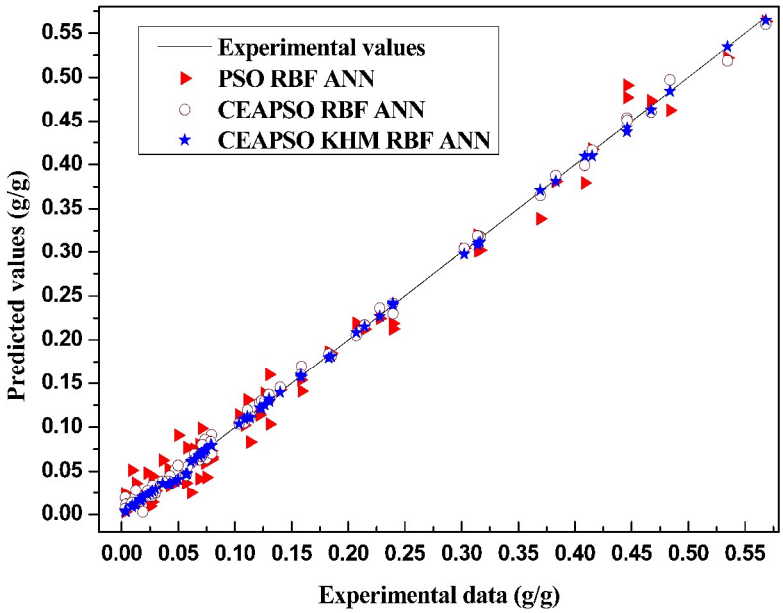

Figure 7. Predicted data VS. experimental data in the testing database

Moreover, several solubility prediction models proposed in recent years are selected as comparative models in order to show the advances and significance of the model in the current work, such as CSPSO-C RBF ANN [34], CSPSO-FC RBF ANN [33], CSPSO-KHM RBF ANN [31]. Table 3 indicates the statistical data of these models.

Table 3. Statistical parameters of the comparison models

Model	*ARD*	R^2	*RMSEP*	*Best Fitness*	*Time* (S)
Model proposed in Ref. [34]	0.1282	0.9970	/	5.96 E-07	/
Model proposed in Ref. [33]	0.1071	0.9973	/	4.78 E-07	16.79
Model proposed in Ref. [31]	0.1051	0.9975	0.0107	4.52 E-07	21.76
Model proposed in this work	0.1001	0.9982	0.0103	3.67 E-07	6.78

In terms of the accuracy and corrections, the CEAPSO KHM RBF ANN model proposed in this article is slightly better and has the lowest deviations than the other models. In terms of the convergence speed, the CEAPSO KHM RBF ANN model is faster, it achieves stable convergence upon the 100th iteration approximately, while the

CSPSO-C RBF ANN [34], CSPSO-FC RBF ANN [33] and CSPSO KHM RBF ANN [31] need approximately 500, 380 and 300, respectively. Importantly, the calculation time is much shorter, about one third of the others. It attributes the shorter calculation time to the training algorithm of the model adopts APSO with rapid convergence speed.

Overall, we can see that both the convergence speed and corrections of the CEAPSO KHM RBF ANN model are superior to the others; the performance of the model in the current work is better and has obvious advantages in predication accuracy and correlation compared with that in their recently published article.

3.3 Discussion and analysis

The results presented in this work show that the proposed model is reliable in predicted the solubility of gas in polymer, has presented its good performance of solubility prediction, and achieves satisfying effect in accuracy, execution time and correlation. It can be known from the comparison with other models that the combination property of the model in this article has significant advantages. The reasons for its excellent performance mainly contain two aspects. On the one hand, the training algorithm of the model adopts APSO with rapid convergence speed, and it also improves the problem of prematurity through chaotic disturbance; on the other hand, the KHM clustering method has made the model training more targeted and purposeful, the center and spread of radial basis function are more reasonable.

In many gas/polymer system, the solubility increases almost linearly with pressure. Take 4 polymers as an example, consisting of PBSA, PP, PVAc and CPEs. Figures 8-11 show the correlations between predicted solubility and experimental data for CO_2/polymer systems at various pressures and temperatures.

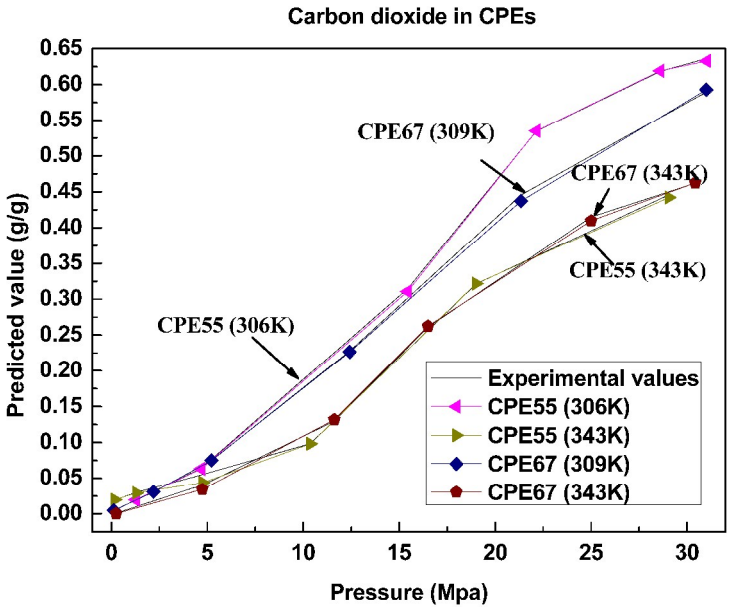

Figure 8. Corrections between predicted values and experimental data (1)

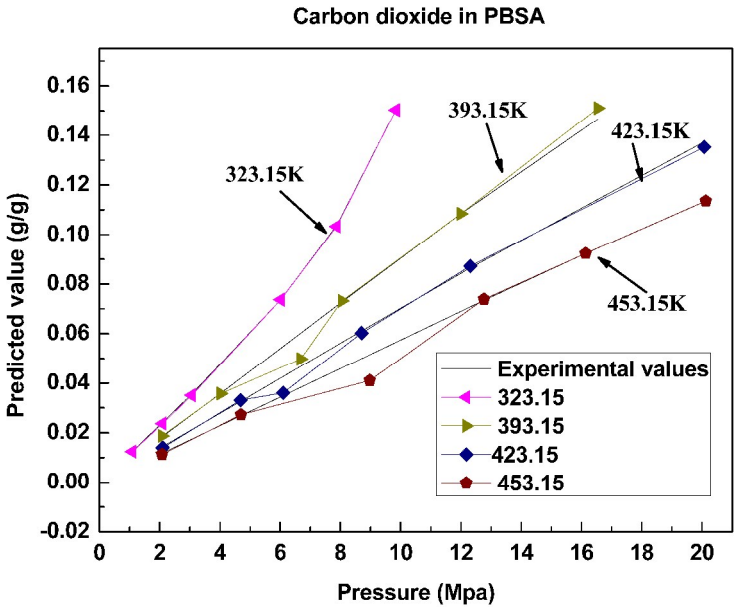

Figure 9. Corrections between predicted values and experimental data (2)

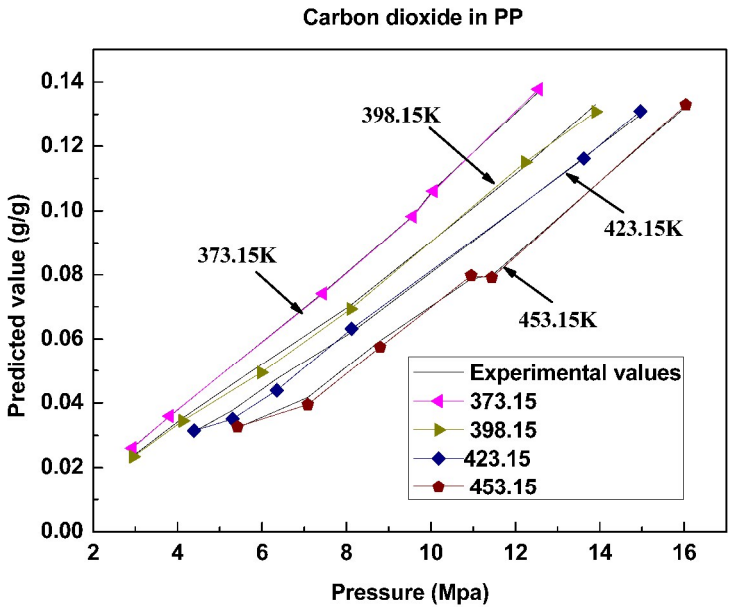

Figure 10. Corrections between predicted values and experimental data (3)

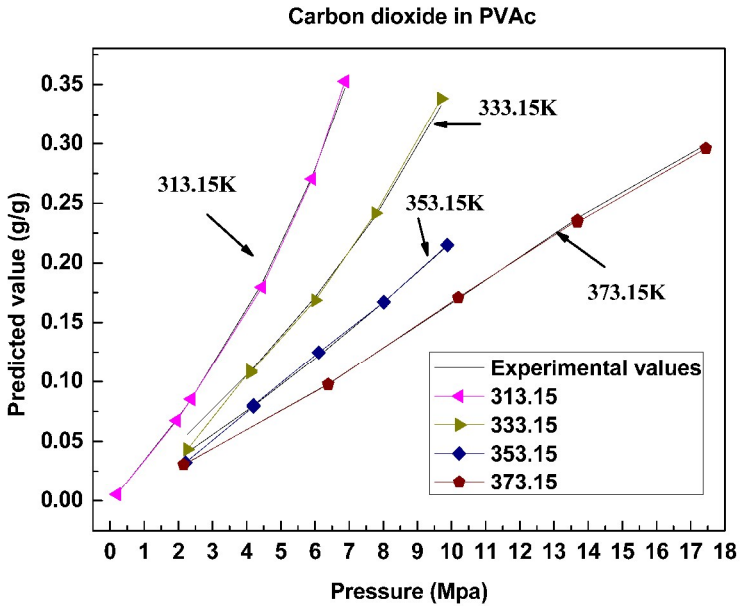

Figure 11. Corrections between predicted values and experimental data (4)

These figures show that the solubility of CO_2 in most polymers increases with increasing pressure and decreasing temperature, it is consistent with the tendency of the solubility experiment. This tendency can be explained by the plasticizing effect. The mobility increases with the increasing pressure because the molecules are forced

between the polymers chains lead to expanding the space between molecules. Once the pressure is further raised, more gas molecules will be absorbed with the increased mobility of the chains. At the same time, the gas density descends with the increasing temperature, which can be correlated with the lower solubility.

4. Conclusion

In order to show the applicability of the proposed model for solubility prediction of carbon dioxide in polymers, a hybrid model called CEAPSO KHM RBF ANN was developed in this work. Through test and comparison, the model's advancement has been proved, and a reliable prediction technique has been provided for research on solubility. The model in this article not only can be used in field of prediction, but can also be expanded to wider application and research field, such as thermodynamics, self-assembly of high polymer materials, kinetic analysis and so forth, so as to analyze chemical characteristics, physical characteristics, mechanical property, rheological properties and other features of various materials. These results in this work should contribute to the enlargement of the database necessary for understanding the phase behaviour of the gas/polymer system, and for the design and optimization of processing techniques.

ABBREVIATIONS

RBF	Radial Basis Function
ANN	Artificial Neural Network
PSO	Particle Swarm Optimization
APSO	Accelerated particle swarm optimization
CEAPSO	Chaos-enhanced accelerated particle swarm optimization
KHM	K-harmonic means

PP	Polypropylene.
PS	Polystyrene.
PVAc	Poly(vinyl acetate)
CPEs	Carboxylated polyesters
PBSA	Poly(butylene succinate-co-adipate)
ARD	Average Relative Deviation
R^2	Squared Correlation Coefficient
MSE	Mean Square Error
RMSEP	Root Mean Square Error of Prediction

References

1. S. L. Liu, L. Shao, M. L. Chua, C. H. Lau, H. Wang and S. Quan, *Prog Polym Sci*, 2013, **38**, 1089-1120.
2. X. Han and M. Poliakoff, *Chem Soc Rev*, 2012, **41**, 1428-1436.
3. Q. Zhang, N. Vanparijs, B. Louage, B. G. De Geest and R. Hoogenboom, *Polym Chem*, 2014, DOI: 10.1039/c3py00971h.
4. Z. G. Lei, C. N. Dai and B. H. Chen, *Chem Rev*, 2014, **114**, 1289-1326.
5. M. Galizia, Z. P. Smith, G. C. Sarti, B. D. Freeman and D. R. Paul, *J. Membr. Sci.*, 2015, **475**, 110-121.
6. M. Fischlschweiger and S. Enders, *Macromolecules*, 2014, **47**, 7625-7636.
7. L. Pogliani and J. V. de Julian-Ortiz, *RSC Adv.*, 2013, **3**, 14710-14721.
8. M. Minelli and M. G. De Angelis, *Fluid Phase Equilibr*, 2014, **367**, 173-181.
9. H. Ziaee, S. M. Hosseini, A. Sharafpoor, M. Fazavi, M. M. Ghiasi and A. Bahadori, *J. Taiwan Inst. Chem. Eng.*, 2015, **46**, 205-213.

10. R. Jalem, M. Nakayama and T. Kasuga, *J Mater Chem A*, 2014, **2**, 720-734.

11. Q. Wang, O. G. Apul, P. F. Xuan, F. Luo and T. Karanfil, *RSC Adv.*, 2013, **3**, 23924-23934.

12. J. S. Torrecilla, C. Tortuero, J. C. Cancilla and P. Diaz-Rodriguez, *Talanta*, 2013, **116**, 122-126.

13. Y. Bakhbakhi, *Math Comput Model*, 2012, **55**, 1932-1941.

14. H. Pahlavanzadeh, S. Nourani and M. Saber, *J Chem Thermodyn*, 2011, **43**, 1775-1783.

15. B. Mehdizadeh and K. Movagharnejad, *Fluid Phase Equilibr*, 2011, **303**, 40-44.

16. F. Gharagheizi, A. Eslamimanesh, A. H. Mohammadi and D. Richon, *Ind Eng Chem Res*, 2011, **50**, 221-226.

17. A. Khajeh and H. Modarress, *Expert Syst Appl*, 2010, **37**, 3070-3074.

18. J. F. Pei, C. Z. Cai, Y. M. Zhu and B. Yan, *Macromol Theor Simul*, 2013, **22**, 52-60.

19. X. Zhao, M. C. Nguyen, C. Z. Wang and K. M. Ho, *RSC Adv.*, 2013, **3**, 22135-22139.

20. J. Luo, W. Lin, X. Cai and J. Li, *Chin J Chem Eng*, 2012, **20**, 950-957.

21. R. Pacheco-Contreras, D. J. Borbon-Gonzalez, M. Dessens-Felix, L. O. Paz-Borbon, R. L. Johnston, J. C. Schon, M. Jansen and A. Posada-Amarillas, *RSC Adv.*, 2013, **3**, 11571-11579.

22. L. Zhuo, J. Zhang, P. Dong, Y. D. Zhao and B. Peng, *Neurocomputing*, 2014, **134**, 111-116.

23. Z. Beheshti and S. M. H. Shamsuddin, *Inform Sciences*, 2014, **258**, 54-79.

24. T. T. Nguyen, Z. Y. Li, S. W. Zhang and T. K. Truong, *Expert Syst Appl*, 2014, **41**, 2134-2143.

25. S. E. K. Fateen and A. Bonilla-Petriciolet, *Ind Eng Chem Res*, 2014, **53**, 10826-10834.

26. X. W. Xia, J. N. Liu and Z. B. Hu, *Appl Soft Comput*, 2014, **23**, 76-90.

27. S. E. K. Fateen and A. Bonilla-Petriciolet, *Fluid Phase Equilibr*, 2014, **375**, 360-366.

28. X. G. Liu and C. Y. Zhao, *Aiche J*, 2012, **58**, 1194-1202.

29. J. A. Lazzus, *Fluid Phase Equilibr*, 2010, **289**, 176-184.

30. M. S. Li, X. Y. Huang, H. S. Liu, B. X. Liu, Y. Wu, A. H. Xiong and T. W. Dong, *Fluid Phase Equilibr*, 2013, **356**, 11-17.

31. M. Li, X. Huang, H. Liu, B. Liu, Y. Wu and L. Wang, *RSC Adv.*, 2015, **5**, 45520-45527.

32. M. S. Li, X. Y. Huang, H. S. Liu, B. X. Liu, Y. Wu and F. R. Ai, *Acta Chim Sinica*, 2013, **71**, 1053-1058.

33. Y. Wu, B. X. Liu, M. S. Li, K. Z. Tang and Y. B. Wu, *Chin J Chem*, 2013, **31**, 1564-1572.

34. M. S. Li, X. Y. Huang, H. S. Liu, B. X. Liu and Y. Wu, *J Appl Polym Sci*, 2013, **130**, 3825-3832.

35. W. B. Wang, Q. Y. Feng and D. Liu, *Prog Electromagn Res*, 2011, **115**, 173-189.

36. C. H. Yang, S. W. Tsai and L. Y. Chuang, *Appl Math Comput*, 2012, **219**, 260-279.

37. A. H. Gandomi, G. J. Yun, X. S. Yang and S. Talatahari, *Commun Nonlinear Sci*, 2013, **18**, 327-340.

38. F. Q. Yang, T. L. Sun and C. H. Zhang, *Expert Syst Appl*, 2013, **40**, 4735-4735.

39. A. Khajeh, H. Modarress and M. Mohsen-Nia, *Iran Polym J*, 2007, **16**, 759-768.

40. Y. Sato, K. Fujiwara, T. Takikawa, Sumarno, S. Takishima and H. Masuoka, *Fluid Phase Equilibr*, 1999, **162**, 261-276.

41. Z. G. Lei, H. Ohyabu, Y. Sato, H. Inomata and R. L. Smith, *J Supercrit Fluid*, 2007, **40**, 452-461.

42. D. C. Li, T. Liu, L. Zhao and W. K. Yuan, *Ind Eng Chem Res*, 2009, **48**, 7117-7124.

43. Y. Sato, T. Takikawa, A. Sorakubo, S. Takishima, H. Masuoka and M. Imaizumi, *Ind Eng Chem Res*, 2000, **39**, 4813-4819.

44. Y. Sato, M. Yurugi, K. Fujiwara, S. Takishima and H. Masuoka, *Fluid Phase Equilibr*, 1996, **125**, 129-138.

45. S. Hilic, S. Boyer, A. Padua and J. Grolier, *J Polym Sci Polym Phys*, 2001, **39**, 2063-2070.

46. Y. Sato, T. Takikawa, S. Takishima and H. Masuoka, *J Supercrit Fluid*, 2001, **19**, 187-198.

47. M. Skerget, Z. Mandzuka, E. Aionicesei, Z. Knez, R. Jese, B. Znoj and P. Venturini, *J Supercrit Fluid*, 2010, **51**, 306-311.

48. G. E. Tsekouras and J. Tsimikas, *Fuzzy Set Syst*, 2013, **221**, 65-89.

49. A. Alexandridis, E. Chondrodima and H. Sarimveis, *IEEE Trans Neural Netw Learn Syst*, 2013, **24**, 219-230.

Figure and table Caption

Figure 1. Results of topology studies for optimal ANN configuration

Figure 2. Predicted data versus experimental data in training set.

Figure 3. Predicted data versus experimental data in validation set.

Figure 4. Predicted data versus experimental data in testing set (1).

Figure 5. Predicted data versus experimental data in testing set (2).

Figure 6. Curve of MSE VS. Epoch

Figure 7. Predicted data VS. experimental data in the testing database

Figure 8. Corrections between predicted values and experimental data (1)

Figure 9. Corrections between predicted values and experimental data (2)

Figure 10. Corrections between predicted values and experimental data (3)

Figure 11. Corrections between predicted values and experimental data (4)

Table 1. Experimental data in this work

Table 2. Values of ARD, R^2 and RMSEP in the testing set

Table 3. Statistical parameters of the comparison models